Optically Controlled Millimeter-wave Switch with Stepped-Impedance Lines

Yutian Zhang [1], Alexander Weiran Pang [1], Martin J. Cryan [1*]

[1] Department of Electrical and Electronic Engineering, University of Bristol, 75 Woodland Rd, Bristol, UK
[*] m.cryan@bristol.ac.uk

Abstract: A photoconductive grounded coplanar waveguide (GCPW) millimeter-wave switch controlled by a single infrared light emitting diode (LED) is presented. By converting a straight GCPW transmission line into an alternating stepped-impedance line structure, the proposed device shows an on-state insertion loss of less than 2.9 dB and an off-state isolation of more than 15 dB over a wide frequency range of 12-30 GHz, with a particularly good RF performance in the K band (18-27 GHz). The required optical power and electrical power of the switch are only 199 mW and 364 mW, repectively. This device also demonstrates an absorptive characteristic with a low reflection coefficient of less than -13.5 dB within this frequency range for both the on and off states. In addition, by employing through-holes for illumination of a silicon superstrate, the proposed device can be fabricated with rapid and low-cost laser-etching and can be easily integrated with other microwave and millimeter-wave circuits.

1. Introduction

Optically controlled attenuation or switching of microwave and millimeter-wave signals has attracted increasing attention partly due to the high linearity and high isolation between signal and control circuitry [1]. Microwave switches based on illumination of a silicon die bridging a microstrip or coplanar waveguide (CPW) inner conductor gap have been extensively investigated in [2-6]. These achieved more than 10 dB switching with either fibre coupled lasers or infrared light emitting diodes (LEDs) below 6 GHz, whereas the off-state isolations quickly deteriorate at higher frequencies due to increased coupling through the gap. The exploitation of the photoinduced plasma regions along CPW gaps to attenuate microwave signals was first reported by Platte [7] where 1.3 dB attenuation up to 20 GHz was obtained on a silicon substrate with an optical intensity of 357mW/cm2. Flemish [8] presented a silicon-based meandered CPW line microwave attenuator which demonstrated more than 20 dB attenuation from 1.5 GHz with the illumination of a single LED. However, the on-state insertion loss of this device starts to increase significantly from 5.9 GHz because of its low pass filter (LPF) characteristic. In the higher portion of the microwave band, a CPW switch in [9] obtained an average 40 dB isolation on a high resistivity (HR) silicon substrate from 2.3-25 GHz with a 65 mW fibre-coupled laser. We recently also reported a grounded coplanar waveguide (GCPW) millimeter-wave switch [10] based on glass substrate and silicon superstrate which obtained an isolation better than 15 dB from 32-50 GHz using a 175 mW fibre-coupled laser. However, the illuminated areas in [9-10] were confined to within the dimensions of 1×1 mm^2 which are difficult to achieve using compact and low-cost LEDs. Moreover, [8-10] required costly and time-consuming optical lithographical fabrication and thus cannot be integrated with typical microwave printed circuit boards (PCBs) directly. In addition, none of [2-10] are completely absorptive (both on-state and off-state return loss (RL) ≥ 10 dB) within their operating frequency bands which may cause problems in many microwave systems such as switched antenna beamforming systems. In this letter, we report on a low-cost LED controlled broad-band photoconductive millimeter-wave absorptive switch which incorporates alternating stepped-impedance GCPW transmission lines [11-12]. This is a type of coplanar slow-wave line which can increase the gap length under illumination for higher signal absorption and attenuation and to our knowledge has not been used in any previous photoconductive microwave or millimeter-wave switch configurations. Although [8] used a meandered CPW line configuration to enhance the signal attenuation below 5.9 GHz, our stepped-impedance GCPW line configuration demonstrates a better on-state (light-off) insertion loss than a meandered GCPW line configuration from 12 – 30 GHz while also providing an improved off-state (light-on) isolation (detailed in Section 2.2.3). This device also features rapid, flexible and low-cost laser-etching fabrication enabling simple integration with other on-board microwave and millimeter-wave circuits.

2. Device Configuration and Modelling

2.1. Device Configuration and RF Model

The layout of the proposed photoconductive millimeter-wave switch is shown in Fig. 1. It is fabricated on a 0.508 mm double-sided Rogers RO4003c laminate with a permittivity of 3.38 and a dissipation factor of 0.0027. GCPW is used in order to allow for integration with other planar transmission lines and lumped electronic devices. The conductive vias arranged along the structure are for spurious transmission mode suppression. A brass block supports the PCB and connectors and also houses a concentrated 940 nm high-power infrared LED [13] with a typical spectrum full width at half maximum (FWHM) of 50 nm via a central through-hole. The central through-hole has the same diameter (D_1=3.2 mm) as the lens of the LED to maintain a relatively high optical intensity without introducing too much optical power loss. After switching on the LED, an illuminated circular area with the same diameter as the brass block hole can be created beneath the PCB and light further passes through a series of closely-arranged non-conductive on-board

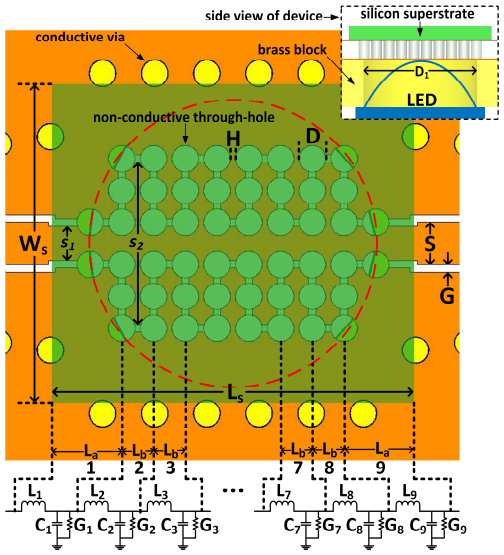

Fig. 1. *Layout and equivalent circuit of the proposed millimeter-wave switch (dashed circle: illuminated area). S = 0.48 mm, G = 0.08 mm, D = 0.3 mm, H = 0.05 mm, L_s = 3.99 mm, W_s = 3.61 mm, D_1 = 3.2 mm, L_a = 0.77 mm, L_b = 0.35 mm*

through-holes (see inset in Fig. 1) to generate plasma regions for signal attenuation in a 400 µm thick passivated HR silicon superstrate which is placed above the PCB. Although the idea of pumping optical power through a PCB by a single drilled hole had been employed in [14], our work differs since we are using multiple through-holes which have a much smaller diameter than the diameter of the entire illuminated area. This enables much more design flexibility and complexity.

Within the capability of our laser-etching machine, G, D and H of the presented device are reduced to 0.08 mm, 0.3 mm and 0.05 mm respectively to minimize the GCPW gap for better light-on attenuation [7] and maximize light transmittance through the PCB. The inner conductor width S of the external GCPW feed line is chosen as 0.48 mm which gives a characteristic impedance of 50 Ω, and the length and width of the silicon superstrate L_s and W_s are set to 3.99 mm and 3.61 mm respectively to enclose the induced plasma regions without introducing too much insertion loss in the on-state.

The alternating stepped-impedance line structure under silicon superstrate can be divided into 9 sections of transmission lines with different characteristic impedances (see the bottom of Fig. 1). Sections 1, 3, 5, 7 and 9 have equal characteristic impedances as is the case for sections 2, 4, 6 and 8. The width of the wide section center conductor, s_2, can be expressed as a function of the narrow section width, s_1, as $s_2 = s_1 + k\mathrm{D} + k\mathrm{H}$ (k = 0, 2, 4…) where k is an indicator of the number of through-holes arranged within the illuminated area. The optimum values for k and s_1 will be discussed in Section 2.2.3.

Since the length of each transmission line section (L_a = 0.77 mm, L_b = 0.35 mm) is far less than the GCPW wavelength at 35 GHz which is our maximum frequency of concern, an approximate equivalent circuit can be derived where each transmission line section is represented by a series inductor, a shunt capacitor and a shunt conductance. This forms a 18th order LPF in the dark state and an attenuator in the illuminated state when all conductances in the circuit are significantly increased.

2.2. *Full-wave Modelling*

2.2.1 Single-layer Model: The three-dimensional modelling of the microwave properties of an optically-induced plasma in silicon was first proposed by [15]. Our previous paper [16] simplified this by modelling the photo-induced plasma region as a multilayer block, assuming a uniform illumination. However, conducting this kind of accurate modelling in full-wave solvers will take a large amount of simulation time and computer memory, especially for complicated structures as used in this paper. We hence adopt a uniform single-layer model for the generated plasma regions which takes less time and memory while maintaining a reasonably good prediction of the measured results.

The full-wave modelling of the device is conducted using CST Microwave Studio software. For a single through-hole, the photoinduced plasma region is modelled as a uniform conductive cylinder in the silicon superstrate with a diameter equal to the through-hole diameter and a height of 177 µm (see inset in Fig. 2) which is the depth where the optical intensity falls to below 5% of its surface value for a 940 nm illumination on silicon [16].

2.2.2 Determination of Plasma Conductivity: The LED used in this paper has a maximum allowable forward current of 1 A (the corresponding electrical power consumption is 2.9 W) which can generate an optical power of 1.31 W when measured from the other side of the brass block hole. However, we focus on a low-power mode of the LED (a forward current of 150 mA, an electrical power consumption of 364 mW and an optical power of 199.43 mW) in order to reduce electrical power consumption.

Assuming a uniform illumination, the light-on optical intensity on the surface of the silicon superstrate can be determined by dividing the measured optical power (199.43 mW or 1.31 W) by the area of illumination ($\pi \times D_1^2/4$), giving

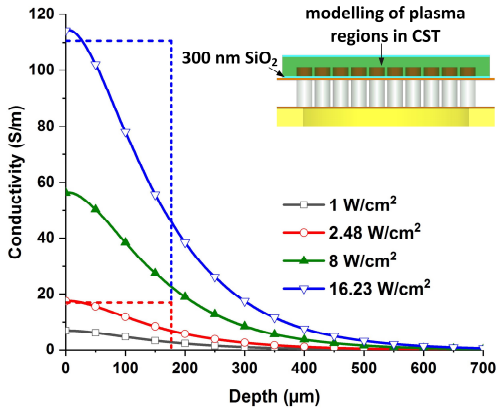

Fig. 2. *Conductivity versus depth in silicon at 940 nm wavelength for various optical intensities (dashed frame: equivalent conductivities of the 177 µm thick plasma regions in CST)*

a value of 2.48 W/cm^2 or 16.23 W/cm^2. Based on our previous work [16], Fig. 2 shows the calculated conductivity versus depth in silicon at a wavelength of 940 nm for these and some other levels of optical intensity. The conductivity of the plasma regions in CST is thus set to maintain the same area as under the 2.48 W/cm^2 curve or the 16.23 W/cm^2 curve on the interval [0, 400] (400 µm is the thickness of the silicon superstrate), giving a value of 16.9 S/m or 110.57 S/m.

2.2.3 Dimension Optimization: Using the value of light-on optical intensity and light-on conductivity obtained for the low-power mode of the LED (2.48 W/cm^2 and 16.9 S/m), the optimization of the dimensions of the proposed switch is carried out.

Fig. 3 demonstrates the effect of different k values on the transmission of the proposed switch in both dark and illuminated states, with s_1 fixed to 0.48 mm initially. As k increases from 0 to 6, better light-on attenuation is attained below 35 GHz due to more plasma regions generated in the illuminated area. However, the LPF characteristic of the device also becomes more significant as the cutoff frequency moves towards lower frequency. We hence choose k = 4 for our design for an on-state coverage of the entire K_u band (12-18 GHz), K band (18-27 GHz) and upper 5G experimental band (24.25-29.5 GHz) with an enhanced off-state isolation compared with the k = 0 and k = 2 configurations, whereas for sub-22GHz applications the k = 6 configuration is most suitable which has best off-state isolation in this range.

The inner conductor width of transmission line sections 1, 3, 5, 7 and 9 is then optimized by setting k to 4 and varying s_1. From Fig. 4 we can see that with a decreasing s_1 the light-on attenuation is slightly improved, whereas the light-off transmission constantly declines above 25 GHz. This suggests an optimum s_1 = 0.48 mm for a trade-off between on-state insertion loss and off-state isolation.

Fig. 5 gives a transmission comparison between the proposed stepped impedance GCPW line switch and a typical meandered GCPW line switch which has a similar configuration to [8] and has identical S, G, D, H and D_1 as the proposed one. The meandered GCPW line switch has a similar on-state insertion loss to the proposed switch and a slightly better off-state isolation up to 12 GHz. However, the on-state insertion loss of the meandered GCPW line switch quickly deteriorates above 15 GHz while our proposed switch maintains both a good on-state insertion loss and a good off-state isolation up to 30 GHz. This suggests our proposed switch is more suitable for applications above 12 GHz compared with a typical meandered GCPW line switch.

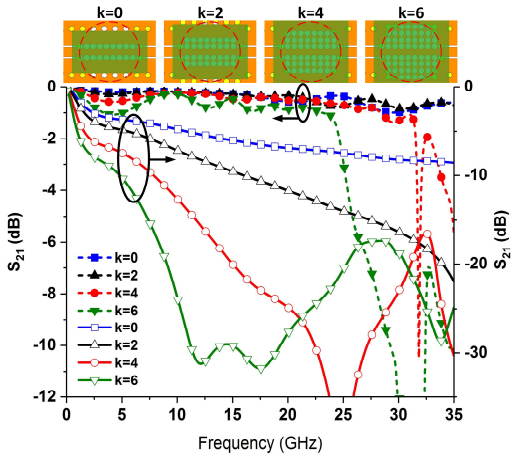

Fig. 3. *Simulated transmission of the proposed switch with various k and fixed s_1 = 0.53 mm (dashed: light-off; solid: light-on)*

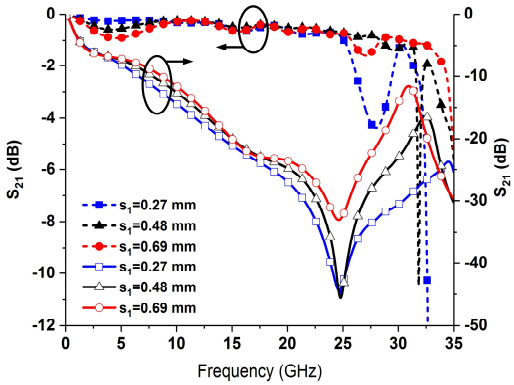

Fig. 4. *Simulated transmission of the proposed switch with various s_1 and k set to 4 (dashed: light-off; solid:light-on)*

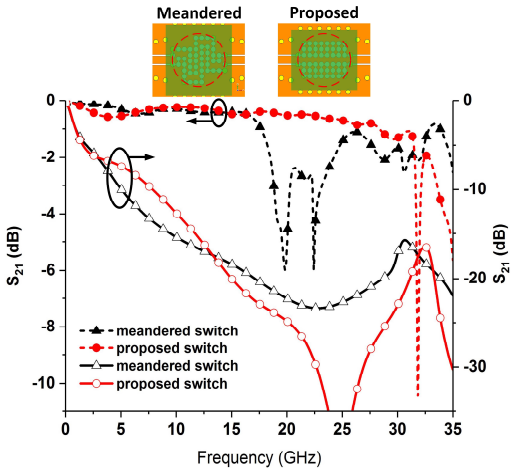

Fig. 5. *Simulated transmissions of the proposed stepped impedance GCPW line switch and a typical meandered GCPW line switch (dashed: light-off; solid:light-on).*

3. Measurements

The fabricated switch was mounted onto a brass block and then soldered with two K connectors. A plastic holder was screwed onto the brass block to hold the silicon superstrate. The LED was powered by a DC supply and S-parameters were measured with an Agilent E8364A network analyzer (see Fig. 6). Fig. 7 and Fig. 8 show the measured transmission and reflection coefficient of the proposed switch for various optical intensities, which correspond to an LED forward current of 0, 150 mA and 1 A respectively.

It can be seen from Fig. 7 that an isolation of at least 15 dB is obtained over a wide frequency range of 12-30 GHz for the optical intensity of 2.48 W/cm^2 or over an extended range of 6.3-30 GHz for the intensity of 16.23 W/cm^2, while

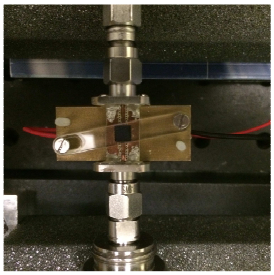

a

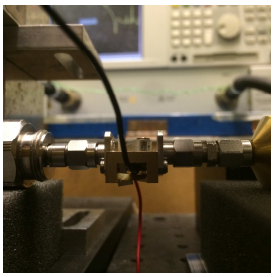

b

Fig. 6. *The measurement setup of the proposed device* ***(a)*** Top view, **(b)** Side view

the light-off insertion loss is constantly below 2.9 dB in these ranges. there is also a good agreement between simulated and measured light-off transmissions until 27.5 GHz, above which the discrepancy is mainly due to the imperfection of PCB fabrication and the variation between the microwave properties of the silicon wafer used in measurement and the material settings of silicon in CST. For light-on transmission, simulation with the single-layer plasma model predicts the general degree of RF attenuation reasonably well throughout 0-35 GHz for both optical intensities. However, a notch near 25 GHz on the simulated 2.48 W/cm^2 curve and a notch near 29 GHz on the simulated 16.23 W/cm^2 curve largely disappear in measurement. This is mostly caused by the existing diffusion tails of the photoinduced plasma regions in measurement which weaken those resonances that are significant in simulation with the single-layer model.

In Fig. 8, as the optical intensity increases, the reflection coefficient of the device increases in general. This partly explains why we choose a low forward current of 150

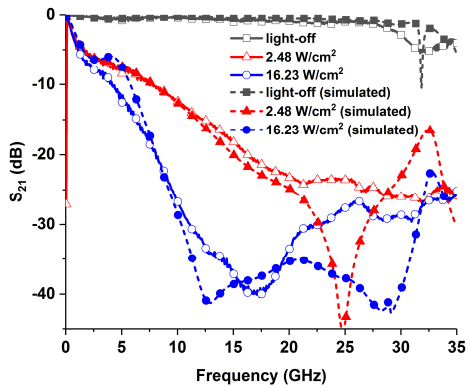

Fig. 7. *Measured S_{21} of the proposed switch for various optical intensities*

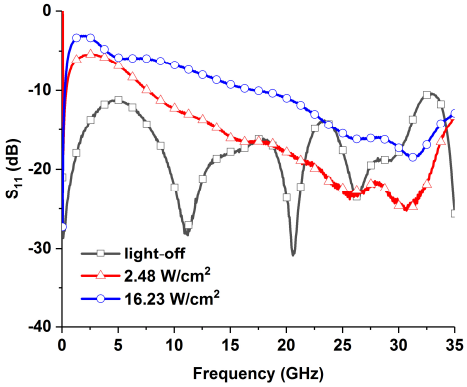

Fig. 8. *Measured S_{11} of the proposed switch for various optical intensities*

mA for the LED (yielding an optical intensity of 2.48 W/cm^2) which is to obtain a trade-off between a -10 dB off-state reflection coefficient and a -15 dB off-state isolation in the entire K_u band. In this situation, the reflection coefficients of the switch are constantly less than -13.5 dB in the range of 12-30 GHz for both the on and off states, which indicates a remarkable absorptive characteristic in this range which is crucial for many microwave and millimeter-wave systems.

Table 1 shows a comparison between the proposed optically controlled millimeter-wave switch and some optically controlled microwave or millimeter-wave switches in references. The switches in [2, 4, 5, 8] are not capable of working above 6 GHz. Compared with works in [9, 10] which can operate at higher frequencies, our proposed switch is the only one which covers the entire K_u band, K band and upper 5G experimental band, with a particularly good RF performance (isolation $\geq$ 21.9 dB, insertion loss $\leq$ 1.1 dB, off-state RL $\geq$ 16.5 dB, and on-state RL $\geq$ 13.8 dB) in the K band. Moreover, our proposed switch is the only one which combines simple laser-etching fabrication and the use of an LED as the light source which is much cheaper and smaller than a fibre-coupled laser over 6 GHz. Although the required optical power of our design is slightly higher than most of the listed switches, our work has the lowest electrical power consumption thanks to the good electrical power utilization of a LED working in the low-power mode. Moreover, our proposed photoconductive switch is the only completely absorptive one within the operating frequency band among the listed switches.

4. Conclusion

We present a single LED controlled GCPW millimeter-wave switch employing an alternating stepped-impedance line structure which increases the off-state isolation significantly while maintaining a good on-state insertion loss over a wide range of 12-30 GHz. The device also has a notable absorptive characteristic in this range which makes it a good candidate for many microwave and millimeter-wave systems (e.g. switched antenna beamforming systems). In addition, the proposed device is fabricated using simple laser-etching techniques and can be directly integrated with other microwave or millimeter-wave circuits.

Table 1 Comparison of optically controlled switches with that proposed in this work

Ref.	Freq. (GHz)	Isolation (dB)	Insertion loss (dB)	Off-state RL (dB)	On-state RL (dB)	Optical power (mW)	El. power (mW)	Light source	Fabrication
[2]	2-6	≥ 12	≤ 1.4	Unknown	Unknown	175	2000	Fibre-coupled laser	Optical lithography
[4]	1-3	≥ 15	≤ 2.3	Unknown	Unknown	Unknown	Unknown	Fibre-coupled laser	Laser-etching
[5]	1-6	≥ 12.5	≤ 2.3	≥ 0.5	Unknown	650	1800	LED	Laser-etching
[8]	1-5.9	≥ 20	≤ 3	≥ 5	≥ 7.5	70	388	LED	Optical lithography
[9]	2.3-25	≥ 20	≤ 1.7	≥ 1.5	≥ 22	65	Unknown	Fibre-coupled laser	Optical lithography
[10]	32-50	≥ 15	≤ 4	Unknown	Unknown	175	2000	Fibre-coupled laser	Optical lithography
Proposed	12-30	≥ 15	≤ 2.9	≥ 13.5	≥ 13.8	199	364	LED	Laser-etching

5. References

[1] Kaneko, T., Takenaka, T., Low, T. S., et al.: 'Microwave switch: LAMPS (light activated microwave photoconductive switch)', Electron. Lett., 2003, 39, (12), pp. 917–919

[2] Pang, A. W., Bensmida, S., Gamlath, C. D., et al.: 'Non-linear characteristics of an optically reconfigurable microwave switch', IET Microw. Antennas Propag., 2018, 12, (7), pp. 1060–1063

[3] Panagamuwa, C. J., Chauraya, A., Vardaxoglou, J. C.: 'Frequency and beam reconfigurable antenna using photoconducting switches', IEEE Trans. Antennas Propag., 2006, 54, (2), pp. 449–454

[4] Lan, L., Zhao, D., Wang, B.: 'Performance Improvement of Optically Controlled Microwave Switch by Introducing Complementary Split-Ring Resonator', IEEE Antennas Wireless Propag. Lett., 2013, 12, pp. 930–932

[5] Kowalczuk, E. K., Panagamuwa, C. J., Seager, R. D.: 'Design and Operation Influences Regarding Rise and Fall Time of a Photoconductive Microwave Switch'. Proc. Loughborough Antennas & Propag. Conf. (LAPC), Loughborough, UK, Nov 2013, pp. 149–154

[6] Zhao, D., Han, Y., Zhang, Q., et al.: 'Experimental Study of Silicon-based Microwave Switches Optically Driven by LEDs', Microw. Opt. Technol. Lett., 2015, 57, (12), pp. 2768–2774

[7] Platte, W., Sauerer, B.: 'Optically CW-induced losses in semiconductor coplanar waveguides', IEEE Trans. Microw. Theory Tech., 1989, 37, (1), pp. 139–148

[8] Flemish, J. R., Haupt, R. L.: 'Optimization of a photonically controlled microwave switch and attenuator', IEEE Trans. Microw. Theory Tech., 2010, 58, (10), pp. 2582–2588

[9] Ali, K. B., Neve, C. R., Gharsallah, A., et al.: 'Photo-Induced Coplanar Waveguide RF Switch and Optical Crosstalk on High-Resistivity Silicon Trap-Rich Passivated Substrate', IEEE Trans. Electron Devices, 2013, 60, (10), pp. 3478–3484

[10] Pang, A. W., Gamlath, C. D., Cryan, M. J.: 'An Optically Controlled Coplanar Waveguide Millimeter-Wave Switch', IEEE Microwave Wireless Compon. Lett., 2018, 28, (8), pp. 669–671

[11] Görür, A., Karpuz, C., Alkan, M.: 'Characteristics of periodically loaded CPW structures', IEEE Microw. Guided Wave Lett., 1998, 8, (8), pp. 278–280

[12] Pozar, D. M.: 'Microwave Engineering' (Wiley Press, 1990, 4th edn. 2012)

[13] LUMILEDS, L1I0-0940060000000 Data Sheet DS191, 2017

[14] Tawk, Y., Albrecht, A. R., Hemmady, S., et al.: 'Optically Pumped Frequency Reconfigurable Antenna Design', IEEE Antennas Wireless Propag. Lett., 2010, 9, pp. 280–283

[15] Gary, R., Arnould, J. D., Vilcot, A.: 'Semi-Analytical Modeling and Analysis in Three Dimensions of the Optical Carrier Injection and Diffusion in a Semiconductor Substrate', Journal of Lightwave Technology, 2006, 24, (5), pp. 2163–2170

[16] Gamlath, C. D., Benton, D. M., Cryan, M. J.: 'Microwave Properties of an Inhomogeneous Optically Illuminated Plasma in a Microstrip Gap', IEEE Trans. Microw. Theory Tech., 2015, 63, (2), pp. 374–383